



# SPECIAL DESIGNED ROUTING DEVICE TO EASE ENDOSCOPIC TRANSFORAMINAL LUMBAR DISC SURGERY: A CADAVERIC STUDY

- Burcu GÖKER<sup>1,2</sup>
- Alican TAHTA<sup>3</sup>
- Ali Güven YÖRÜKOĞLU<sup>4</sup>
- Mehmet Osman AKÇAKAYA<sup>1,2</sup>
- Fahir ŞENCAN<sup>1,2</sup>
- Aydın AYDOSELİ<sup>5</sup>
- Altay SENCER<sup>5</sup>
- Talat KIRIŞ<sup>1,2</sup>
- Ali Tuncay CANBOLAT<sup>5</sup>

<sup>1</sup>Department of Neurosurgery, Liv Hospital, Istanbul/Turkey

<sup>2</sup>Department of Neurosurgery, Istinye

<sup>3</sup>University Medical Faculty, Istanbul/Turkey

Department of Neurosurgery, Medipol University Medical Faculty, Istanbul/Turkey

<sup>4</sup>Department of Neurosurgery, Avrasya Hospital, Istanbul/Turkey

<sup>5</sup>Department of Neurosurgery, Istanbul School of Medicine, Istanbul University, Istanbul/Turkey

#### ORCID NUMBERS:

Burcu Göker: 0000-0002-6084-8690

Ali Can Tahta: 0000-0003-0467-7521

Ali Güven Yörükoğlu: 0000-0002-2388-5839

Mehmet Osman Akçakaya:

0000-0001-8617-202X

Fahir Şencan: 0000-0001-5519-5560

Aydın Aydoseli: 0000-0002-4695-8295

Altay Sencer: 0000-0001-9925-5422

Talat Kırış: 0000-0002-2985-3758

Ali Tuncay Canbolat: 0000-0001-6229-2721

\*Ethics committee approval was obtained for the study.

\*Level of Evidence: Level IV

\*Field of the study: Minimal Invasive Surgery

**Corresponding Author:** Burcu Göker, MD  
Liv Hospital Ulus, Ahmet Adnan Saygun Ave.  
Canan Street, no: 5, Besiktas, Istanbul/Turkey  
**E-mail:** burcugoker79@yahoo.com

**Phone:** 02129998099, Fax: 02129998291

**Received:** 06<sup>th</sup> january 2019

**Accepted:** 01<sup>st</sup> june 2019

#### ABSTRACT

**Background Data:** Fully endoscopic lumbar disc (FELD) surgery via transforaminal (TF) approach may be more demanding to adopt for surgeons experienced with conventional microdiscectomy, due to the necessity of a new anatomic orientation and understanding. We designed a routing device to facilitate access to safe anatomic triangle defined by Kambin at the level of foramen in cadavers.

**Purpose:** To show that the transforaminal route for endoscopic lumbar disc herniations is safely applicable with the aid of a new routing device.

**Materials and Methods:** Ten cadavers between the ages 18-75, with no history of lumbar spinal surgery or trauma, with previous abdominal computed tomography (CT) scans included in our study. Postmortem abdominal CT scans were performed. Images were examined and transforaminal entrance angles without causing damage to retroperitoneal structures for each lumbar disc space and anatomical differences were recorded. TF approach was performed in cadavers using the angles measured from abdominal CTs and the entry point determined with the help of routing device.

**Results:** L1-L2, L2-L3, L3-L4, L4-L5 disc spaces were operated in ten cadavers. Kambin's triangle was successfully reached with help of routing device using data obtained from CT (X',  $\alpha$ ) and C-arm fluoroscopy (X, Y, Y'). Y' marker with protractor on routing device, and the metal rod on this Y' marker with an opening through which only the puncture needle could pass were very important in reaching the target. The metal bar horizontal movement and fixation to this mechanism contributed to operation of device. Entrance points and angles calculated with the help of CT scans were found to be compatible with the images obtained from fluoroscopy and endoscopy during operation.

**Conclusions:** In this study, it has been showed that TF approach can be safely performed with help of the new designed routing device.

**Key Words:** Spinal endoscopy; transforaminal, minimal invasive spine surgery; exiting root, traversing root; endoscopic anatomy

#### INTRODUCTION

Surgery for lumbar disc herniation can be classified into two categories: conventional versus minimally invasive surgery<sup>(10)</sup>. Currently, conventional microdiscectomy (MD) is widespreadly used<sup>(13)</sup>. However, minimally invasive techniques have been increasingly applied all around the world<sup>(3)</sup>. Fully endoscopic lumbar disc surgery (FELD) via TF approach is a minimally invasive technique with advantages of small incision, rapid recovery, short operation time, and low cost<sup>(2)</sup>. For neurosurgeons who are experienced in conventional

MD, the interlaminar approach is easier to adopt because of similarities in the anatomic orientation. However, the lateral TF approach may be more demanding. The initial stage of spinal cannula insertion under fluoroscopy is of the utmost importance, as it leads the surgeon to the optimal target point. Failures at that stage may result in improper placement of the endoscope, creating a risk of nerve root injury and inability to remove the herniated disc. TF approach requires multiple punctures under fluoroscopy as in other minimally invasive spinal surgeries<sup>(9)</sup>.

Transforaminal steroid injection is a common method used in the management of radicular pain. Inexperienced surgeons may perform transforaminal steroid injections to improve foraminal puncture for endoscope placement. However, this may lead to increased exposure to radiation, prolonged operation time, and damage to soft tissue<sup>(3)</sup>. Therefore, we designed a routing device to reduce the number of punctures even in inexperienced hands. In this study, we aimed to evaluate the effectiveness of this routing device which facilitates access to safe anatomic triangle defined by Kambin at the level of foramen in cadavers.

## MATERIALS AND METHODS

The study was approved by the local Institutional Review Board of Istanbul University and Republic of Turkey, Forensic Medicine, Ministry of Justice. This study was conducted in autopsy training hall of Forensic Medicine Institution Morgue Department, Ministry of Justice, Republic of Turkey. Postmortem abdominal CT scans were performed one each cadaver. CT images were examined and TF entrance angles without causing damage to retroperitoneal structures for each lumbar disc space and anatomical differences were recorded.

After the examination of forensic experts and the completion of the autopsy, fresh cadavers were taken to the autopsy training hall. The cadavers were placed in prone position on a radiolucent table. Roller cushions were located bilaterally between shoulder and anterior superior iliac wing. Endoscopic unit and monitor were positioned on the head side, C-arm and surgical instruments were located on foot site, and the surgeon was positioned on the left side of the cadaver.

### **Routing Device:**

A routing device was designed to facilitate access to the secure anatomic triangle defined by Kambin without damaging retroperitoneal structures. This device consisted of following parts (Figure 1, 2, 3);

1. 25x25-cm stainless steel table welded with M8x36 mm stainless steel bolt in the center.
2. U-channel joint (10 cm long, 1.2 cm in diameter; 4.5 cm long, 0.8 cm in diameter in the middle) threaded to the M8x36 mm stainless steel bolt.
3. A 1.2 cm diameter, 85 cm long stainless steel bar passed through the U-joint to form the Y axis of the device (The 8mm flat end side of this bar which was inserted into the

channel joint was fixed with a M6x28 mm stainless steel bolt. One side of the bar was flattened to fix the markers on the Y-axis of the routing device at 90°, and a strip ruler was fixed on it with M6x9 mm setscrew bolt and Plexiglas holder (polymethylmethacrylate based, radiolucent, thermoplastic material. Y axis could stay at 90° as well as it could be moved forward or backward from the open ends (Z axis) of U-joint).

4. A metal rod of 1.2 cm in diameter, 30 cm in length, which could be moved in the Y-axis and used as the X-axis, placed perpendicularly to the Y-axis, and 90° angled, 20x20x40 mm stainless steel axis fixing piece to fix it in the Y-axis 90° with holes 1.2 cm in diameter and M6 teeth to secure both axes (The metal bar forming the X-axis had a strip ruler on it, fixed with M6x9 mm setscrew bolt and Plexiglas holder.

5. 2.4 cm wide, 1.46 cm thick, 12 cm long Plexiglas with a '+' shaped stainless steel marker fixed to the end, attached perpendicularly to the X axis in the Z axis, and secured with stainless steel wing bolt. This Plexiglas was used as an X marker.

6. Markers moving on the Y axis, and perpendicular to this axis, markers mounted on the Z axis, which were secured with M6 stainless steel wing bolt;

- a. 2.4 cm wide, 1.46 cm thick, 12 cm long Plexiglas with '+' shaped stainless steel marker placed on the tip of it (This Plexiglas was used as '0' zero point or Y marker).

- b. A 12 cm long Plexiglas that could move in the Y-Axis and could be attached to the Z-axis with a stainless steel wing bolt, with a goniometer in the end (A goniometer parallel to the X-axis was fixed perpendicular to the lower edge of the free end of this Plexiglas, which was used as the Y' marker. A second Plexiglas of 1.6 cm in length which had a space in it to allow the passage of the metal bar through, was secured by a bolt to allow movement to the backward Plexiglas on the lower edge of goniometer. A metal rod of 0.6 cm in diameter and 20 cm in length was inserted in second Plexiglas, and secured with stainless steel bolt. This metal rod could measure angles, and move back and forth in the second Plexiglas. There was an opening of 1.2 mm diameter, 25 cm long in the middle of metal rod. 18-gauge needle could pass from this opening. So, it is ensured that the target of the needle sent through the metal bar was not deviated.)

The sizes of the Plexiglasses used for the X, Y, Y' markers in the routing device were the same and the sign of each intersected at a point on the Z axis, which formed our target point.

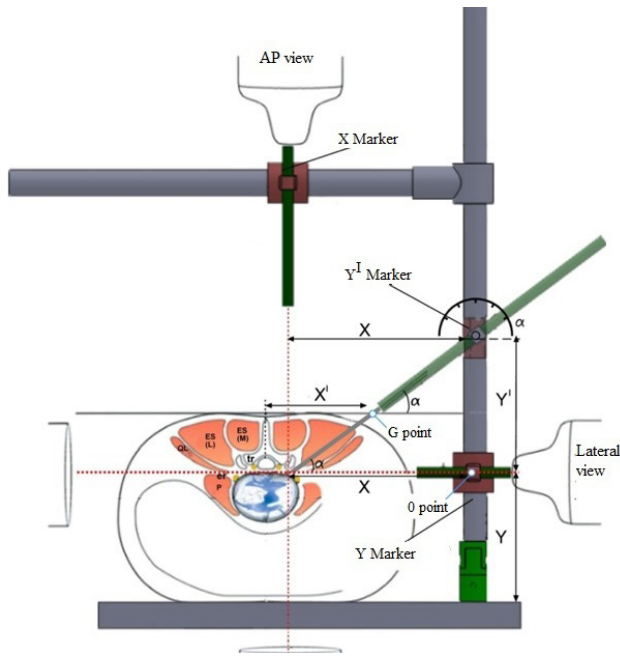


**Figure-1.** This is the demonstrative view of the patient and routing device. X value is distance between midpedicular line and Y axes of the routing device. Y value is distance between Y marker and metal base of the routing device. It will change according to age, gender, weight and height Y' value is obtained by multiplying tangent  $\alpha$  and X value. As tangent  $\alpha$  is a constant value, with increase and decrease of X values, Y' also will increase and decrease. X' value is distance from the entry point to the midline.



**Figure-3.** The metal rod acting on Y-axis and placing perpendicularly to the Y- axis and is going to be used as X-axis (left). The X marker is located at the X axis and placed perpendicularly to the Z axis (right). The X and Y markers are composed of plexyglass at which plus shaped stainless steel is placed to the distal parts (middle).



**Figure-2.** Picture showing the routing device, that is designed according to basic principles of endoscopic transforaminal lumbar disc surgery (AP and antrolateral view: Left and middle respectively). The routing device includes stainless steel bolt at the mid-point of the stainless steel table. U-channel joint is placed in this bolt. The stainless steel rod forms Y axis and passes through the U-channel joints. One side of the Y axis rod is flat in order to have markers stabilized on the rod at 90°. On the other side of the rod, a ruler is placed to make measurements (right).

### **Foraminal puncture with the use of the routing device:**

The routing device was placed under the roller cushions after the positioning of cadaver. Before X and Y axes were determined, the device was moved in the Z axis in the lateral view of C-arm to position it parallel to vertebral end plates. A longitudinal line connecting the spinous processes in the AP image was drawn with the help of a metal rod and the midline was identified. The distances of entrance points from the midline were measured with ruler in cm (Figure 4).

The X marker on the X axis was brought on midpedicular line of target disc space in AP image. The distance of midpedicular line to Y-axis of routing device was recorded as an X value (Figure 4).

In the lateral view, target foraminal level was identified with the Y marker. The distance from this point to the device's plane was recorded as the Y value, and the Y marker was fixed on the Y axis. Also, this point was taken as the Y-axis zero-point (0) for each cadaver (Figure 4).

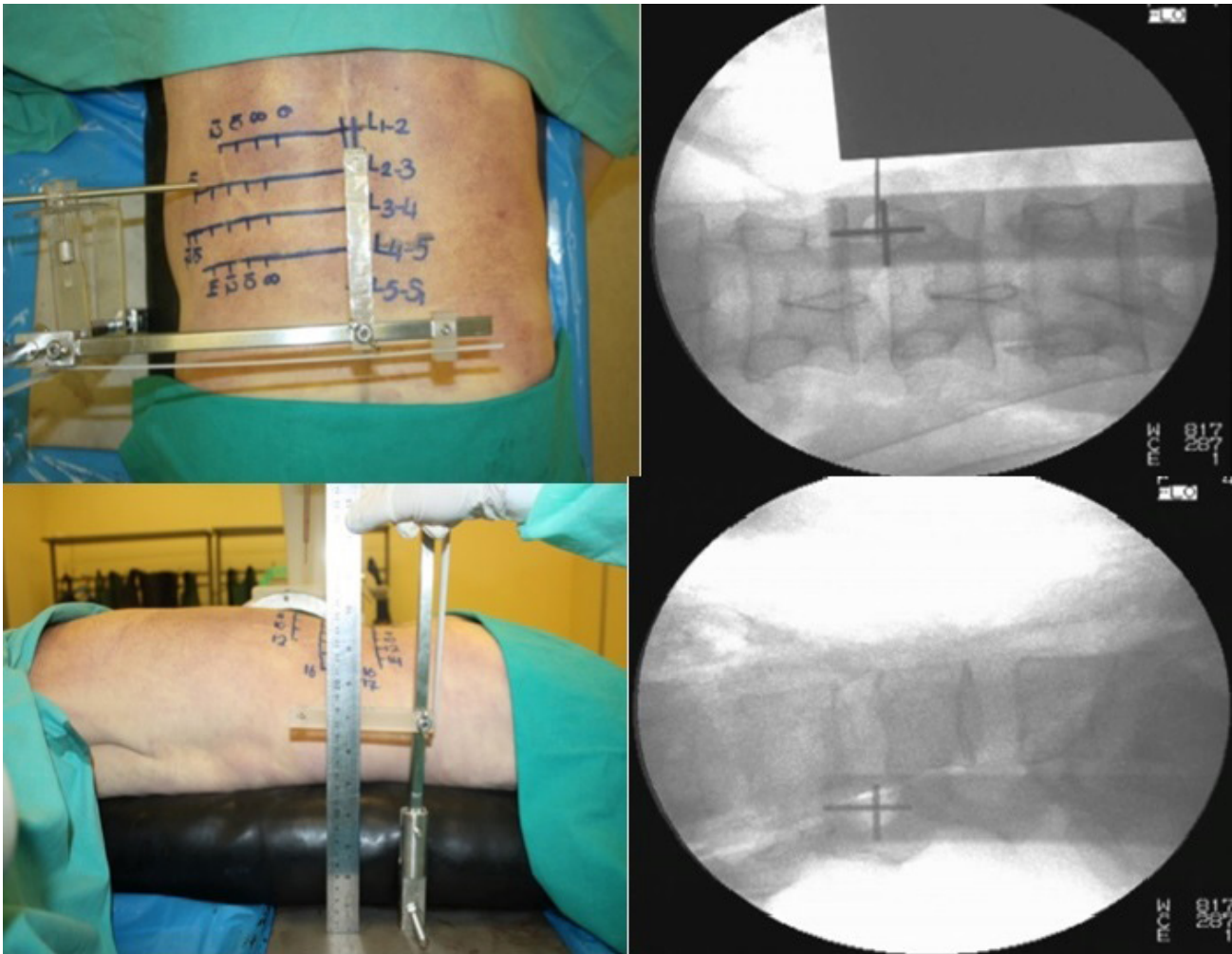


**Figure-4.** Determining the X value at the L2-L3 level X= 23 cm. X marker is placed on to the midpedicular line at the target disc level in AP projection. Distance between midpedicular line and Y axis of the routing device is determined as X value (above row left and right). In the lateral projection Y marker is fastened at the target foramen L2-L3, Y=17.3 cm. Target foraminal levels determined by Y marker at the lateral projection . Distance between Y marker and metal base of the routing device is named as Y value. Y marker is fastened on Y axis and this point is determined as "0" (zero) point (below row left and right).

Safe entrance angle to foramen without damage to retroperitoneal structures ( $\alpha$ -angle) was calculated from abdominal CTs of each cadaver. Disc slope line to enter the target disc space was drawn in sagittal plane with use of axial and sagittal reconstructed abdominal CT images (**Figure 5**). The view of this slope line in axial plane was placed in prone position in CT. A transverse line was drawn at the level of annulus of the target disc space. The angle between the line passed from entrance point on the skin to midpedicular point at the level of foramen without damaging retroperitoneal structures and the transverse line passed from annulus was recorded as the  $\alpha$ -angle.) Y value was obtained by multiplying the tangent  $\alpha$  and X values. The Y' marker was fixed on the Y axis by moving away from the Y marker (zero point) by Y'. The special mechanism on the Y' marker was set as an  $\alpha$ -angle. The entrance point on the skin of the punch needle in this direction (with  $\alpha$ -angle) was identified as the 'G' point. The distance between the midline and G point was measured as X' (**Figure 5**). X' and Y' values were measured

separately for each distance (L1-L2, L2-L3, L3-L4, L4-L5) under C-arm fluoroscopy using the angles obtained from CT with this routing device. Foramen was punctured with the 18-gauge needle that passed through the Y' marker at each disc distance. Needle was seen on midpedicular line in AP view and posterior vertebral line in lateral view (Kambin's triangle) of fluoroscopy (**Figure 5**).

Since it was known that exiting root was the most likely injured anatomical structure during placement of the oval cannula in TF approach, exiting roots from the L1, L2, L3, L4, L5 foramina of 4 cadavers were macroscopically examined while the cannula of endoscope was still in the foramen. The 30-cm long incision that was 6 cm off from midline was made. Skin, subcutaneous tissue, and fascia of paravertebral muscle were passed, and transverse processes were recognized after removal of erector spinae muscles. After excision of intertransverse ligament between transverse processes, quadratus lumborum and psoas muscles were retracted, and the emerging roots were revealed (**Figure 6**).

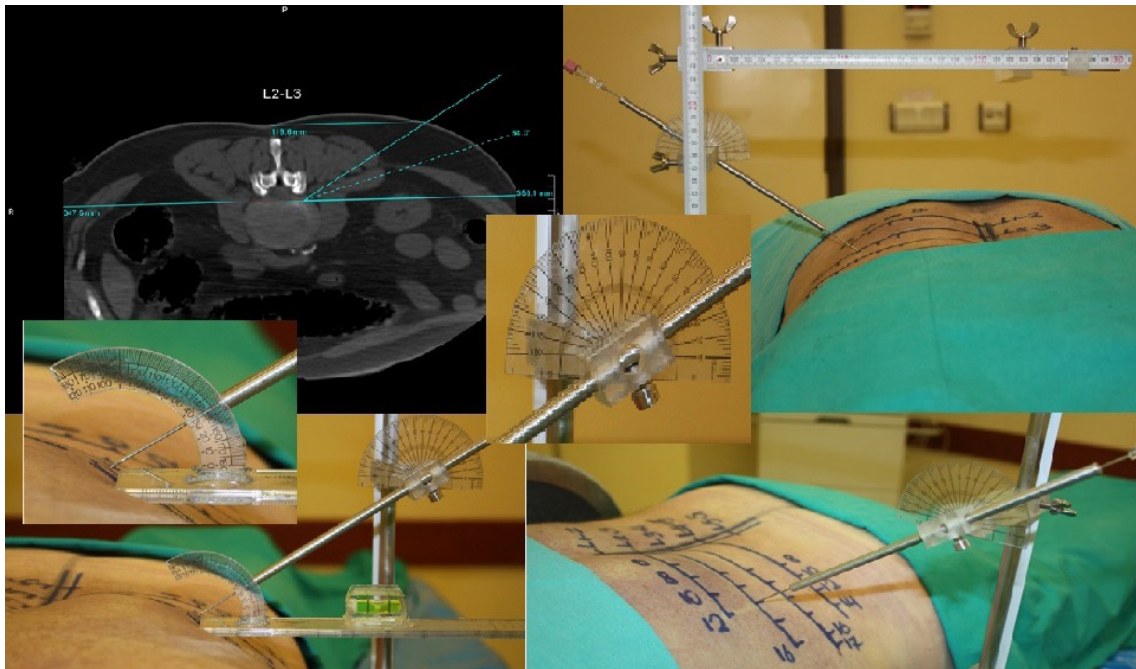


**Figure-5.** Calculation of the entry point to left L2 foramen at L2-3 level from the abdominal CT  $\alpha=34^\circ$ ,  $X'=11.96\sim 12\text{cm}$ . Cadavers' abdominal CT scans were studied and a safe angle is calculated to protect the retroperitoneal structures for every lumbar disc segment (above left). Entry at L2-L3 level to left L2 foramen. Entry angle is  $34^\circ$  and this value is calculated using abdominal CT. By multiplying tangent  $\alpha$  and X value, Y' value is obtained. At the Y axis, the Y' marker is transferred from Y marker to the Y' value and stabilized. Protractor on Y' marker is positioned to the  $\alpha$  angle value. The puncture needle is directed through this angle and entry point on the skin is named as 'E' point. The distance from the E point to the midline is defined as X' value. This figure depicts the entry of the needle on the Y' marker with a  $34^\circ$  angle which is calculated using abdominal CT. The entry point is L2-L3 level at left L2 foramen (above right). Y' is positioned to the  $34^\circ$  at the protractor and at this angle entry point was seen. This was controlled with water scales ruler which included protractor (below left). Skin entry at the X' distance, measured at the abdominal CT, when the X, Y, Y' markers were stabilized and entry angle direction was provided ( $X'=12\text{cm}$ ). After stabilizing X, Y, Y' markers and providing entry angle, it confirmed same skin entry site at X' distance as measured by abdominal CT (below right).

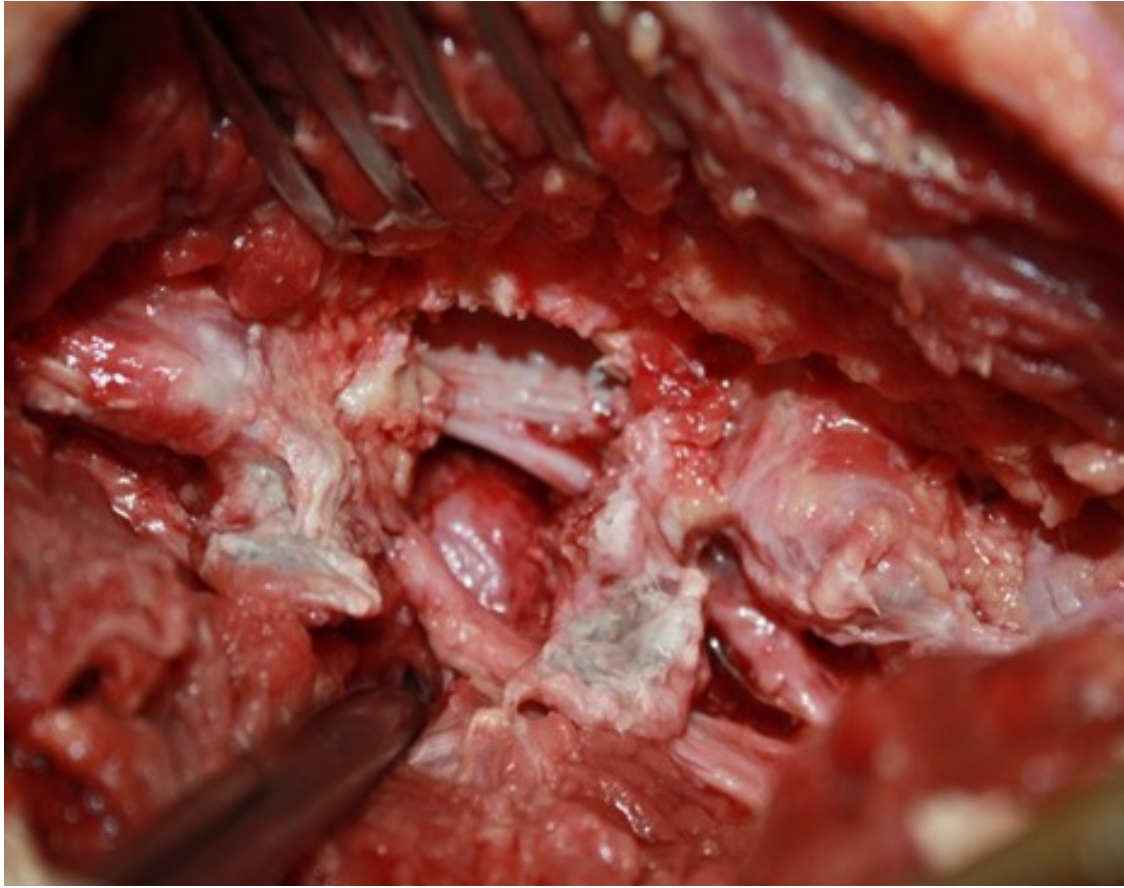


**Figure-6.** The triangular working zone described by Kambin, is bordered medially by the traversing root and the dural sac, inferiorly by the proximal plate of the inferior lumbar segment and anteriorly by the exiting root. Picture showing oval cannula in the triangular working zone. Opening of the oval cannula faces upwards at entry and while passing through the exiting root then it was converted downwards at the foraminal annulus.

## RESULTS

This study was conducted in autopsy training hall of Forensic Medicine Institution Morgue Department, Ministry of Justice, Republic of Turkey. All fresh cadavers had no previous spine trauma or surgery. They were between the ages of 18-75. There were 10 cadavers (3 women, 7 men) in this study. Cadavers' ages ranged between 18-75, the mean age was 53.

The following results were obtained for the distance from midline and entrance angle using a safe way without damage to the retroperitoneal structures when the foramen was targeted at L1-L2, L2-L3, L3-L4, L4-L5 disc spaces in the examinations made on abdominal CTs of fresh cadavers. L5-S1 disc space had been excluded because this space could only be accessed only in one cadaver. The gender, age, weight of the cadavers and the findings obtained from abdominal CTs

and routing device for each disc space were recorded (**Table 1**).

When we look at the values in Table 1, it is seen that X, Y, X', Y' parameters change according to individual differences such as age, sex, height and weight and these values could not be standardized. However, it was seen that in upper levels such as L1-2, L2-3, distance from midline was shorter and the foraminal entrance angle was increased compared to L3-L4, L4-L5 levels (**Table 2**).

The data obtained from these calculations was applied to fresh cadavers using the routing device we developed. We found that target disc space could be reached safely and easily from C-arm fluoroscopy images taken during intervention, and late endoscopic evaluations (**Figure 7, 8**).

**TABLE 1**

|                | <b>Gender</b> | <b>Age</b> | <b>Weight</b> | <b>Disc Level</b> | <b>X'</b> | <b>Angle</b> | <b>X</b> | <b>Tang. Angle</b> | <b>Y'</b> | <b>Y</b> |
|----------------|---------------|------------|---------------|-------------------|-----------|--------------|----------|--------------------|-----------|----------|
| <b>Case 1</b>  | M             | 71         | 78kg          | L1-L2             | 8         | 35           | 18,4     | 0,7002             | 12,8      | 16       |
|                |               |            |               | L2-L3             | 10        | 30           | 18,6     | 0,5774             | 13,5      | 15,8     |
|                |               |            |               | L3-L4             | 11        | 32           | 20,0     | 0,6249             | 16,1      | 14,8     |
|                |               |            |               | L4-L5             | 16        | 18           | 17,2     | 0,3249             | 7,6       | 14,6     |
| <b>Case 2</b>  | M             | 60         | 56kg          | L1-L2             | 8         | 35           | 18,1     | 0,7002             | 12,60     | 17       |
|                |               |            |               | L2-L3             | 10        | 32           | 18,2     | 0,364              | 6,62      | 16,8     |
|                |               |            |               | L3-L4             | 11        | 30           | 17,4     | 0,7002             | 12,1      | 15,3     |
|                |               |            |               | L4-L5             | 12        | 26           | 18,1     | 0,8391             | 15,1      | 14,7     |
| <b>Case 3</b>  | M             | 51         | 60kg          | L1-L2             | 10        | 36           | 21,2     | 0,7265             | 15,4      | 17,7     |
|                |               |            |               | L2-L3             | 12        | 34           | 23,0     | 0,6745             | 15,5      | 17,3     |
|                |               |            |               | L3-L4             | 12        | 30           | 21,1     | 0,5774             | 15,3      | 17       |
|                |               |            |               | L4-L5             | 12        | 30           | 17,0     | 0,5774             | 9,8       | 16,9     |
| <b>Case 4</b>  | M             | 72         | 71kg          | L1-L2             | 10        | 36           | 16,8     | 0,7265             | 12,2      | 20       |
|                |               |            |               | L2-L3             | 10        | 33           | 16,3     | 0,6494             | 10,5      | 18,8     |
|                |               |            |               | L3-L4             | 12        | 24           | 16,5     | 0,4452             | 7,3       | 17,6     |
|                |               |            |               | L4-L5             | 14        | 20           | 17,7     | 0,8391             | 14,7      | 17,3     |
| <b>Case 5</b>  | M             | 31         | 79kg          | L1-L2             | 8         | 43           | 20,0     | 0,9325             | 18,6      | 18,8     |
|                |               |            |               | L2-L3             | 10        | 37           | 21,0     | 0,7536             | 15,8      | 18,2     |
|                |               |            |               | L3-L4             | 14        | 26           | 19,4     | 0,4877             | 9,4       | 17,2     |
|                |               |            |               | L4-L5             | 12        | 28           | 19,0     | 0,5317             | 10,1      | 17       |
| <b>Case 6</b>  | F             | 45         | 75kg          | L1-L2             | 9         | 34           | 16,0     | 0,6745             | 10,7      | 22,7     |
|                |               |            |               | L2-L3             | 10        | 30           | 15,0     | 0,5774             | 8,6       | 20,7     |
|                |               |            |               | L3-L4             | 12        | 18           | 14,6     | 0,3249             | 4,7       | 19,8     |
|                |               |            |               | L4-L5             | 12        | 20           | 13,7     | 0,364              | 4,9       | 19,7     |
| <b>Case 7</b>  | M             | 75         | 80kg          | L1-L2             | 11        | 24           | 23,0     | 0,4452             | 10,2      | 21,3     |
|                |               |            |               | L2-L3             | 12        | 18           | 21,0     | 0,3249             | 6,8       | 21       |
|                |               |            |               | L3-L4             | 10        | 30           | 20,0     | 0,5774             | 11,5      | 20       |
|                |               |            |               | L4-L5             | 14        | 20           | 18,0     | 0,364              | 6,5       | 19,8     |
| <b>Case 8</b>  | F             | 52         | 65kg          | L1-L2             | 11        | 28           | 19,0     | 0,4663             | 8,8       | 18,4     |
|                |               |            |               | L2-L3             | 12        | 26           | 19,2     | 0,364              | 6,9       | 18,2     |
|                |               |            |               | L3-L4             | 13        | 20           | 18,0     | 0,4663             | 8,3       | 17,6     |
|                |               |            |               | L4-L5             | 14        | 18           | 18,1     | 0,4663             | 8,4       | 17,5     |
| <b>Case 9</b>  | F             | 35         | 53kg          | L1-L2             | 10        | 35           | 16,8     | 0,7002             | 11,7      | 18       |
|                |               |            |               | L2-L3             | 10        | 32           | 16,6     | 0,6249             | 10,3      | 17,8     |
|                |               |            |               | L3-L4             | 14        | 26           | 16,2     | 0,4877             | 7,9       | 17,5     |
|                |               |            |               | L4-L5             | 14        | 21           | 16,0     | 0,3839             | 6,1       | 17       |
| <b>Case 10</b> | M             | 37         | 60kg          | L1-L2             | 8         | 35           | 18,5     | 0,7002             | 12,9      | 18       |
|                |               |            |               | L2-L3             | 10        | 32           | 18,1     | 0,6249             | 11,3      | 17,6     |
|                |               |            |               | L3-L4             | 10        | 26           | 17,7     | 0,4877             | 8,6       | 17       |
|                |               |            |               | L4-L5             | 10        | 20           | 17,5     | 0,364              | 6,3       | 16,8     |

**TABLE 2**

| Disc Level | Mean Angle | Mean Distance (X') cm |
|------------|------------|-----------------------|
| L1-L2      | 34.1°      | 9,3                   |
| L2-L3      | 30.4°      | 10,6                  |
| L3-L4      | 26.2°      | 11,9                  |
| L4-L5      | 22.1°      | 13                    |

Recognition and retraction of exiting nerve root was easier in L3-L4 and L4-L5 disc spaces compared with L1-L2 and L2-L3 disc spaces. For this reason, exiting roots from the L1, L2,

L3, L4, L5 foramina of 4 cadavers were macroscopically and endoscopically examined while the cannula of endoscope was still in the foramen. Although the foramina were larger at the upper lumbar levels, it was observed that the root diameter was smaller and the angle between root and dura mater was narrower. So, we think that nerve root damage would be more possible in upper levels (L1-L2, L2-L3) than lower levels (L3-L4, L4-L5). It was observed that traversing root damage occurred in the disc spaces of upper levels during removal of LLP for adequate decompression and exposure of traversing root.

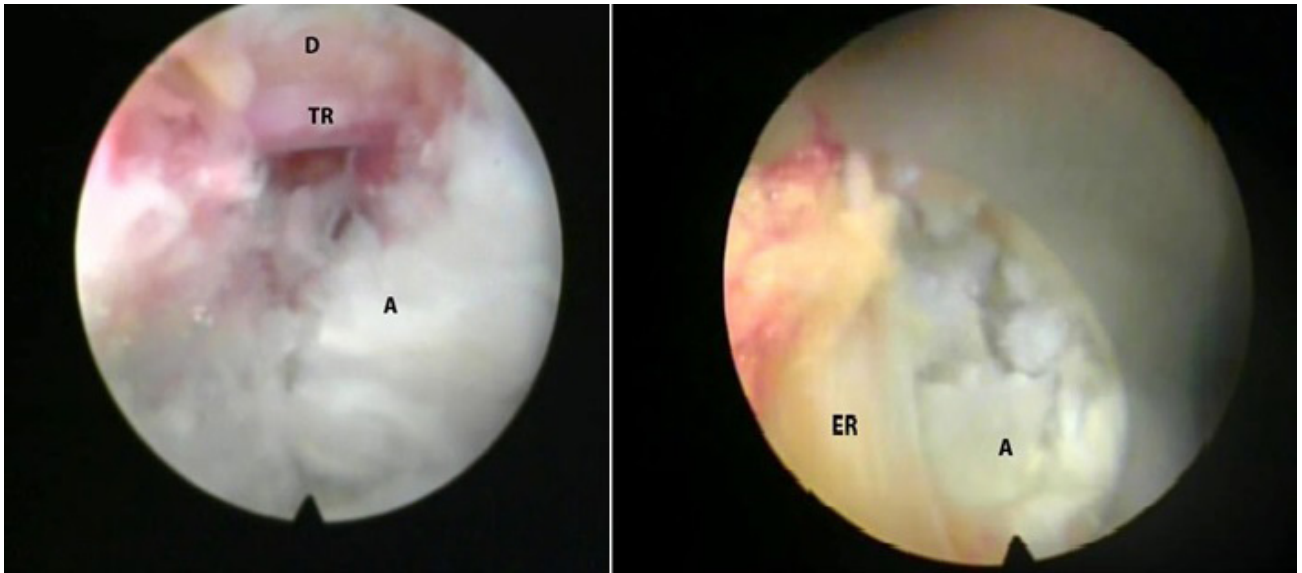


**Figure-7.** When the oval cannula is moved little backward and its tip is positioned cranially at the extraforaminal area, exiting root is observed. We have seen that puncture point and access angle calculated via CT scans were consistent with the fluoroscopic and endoscopic images.

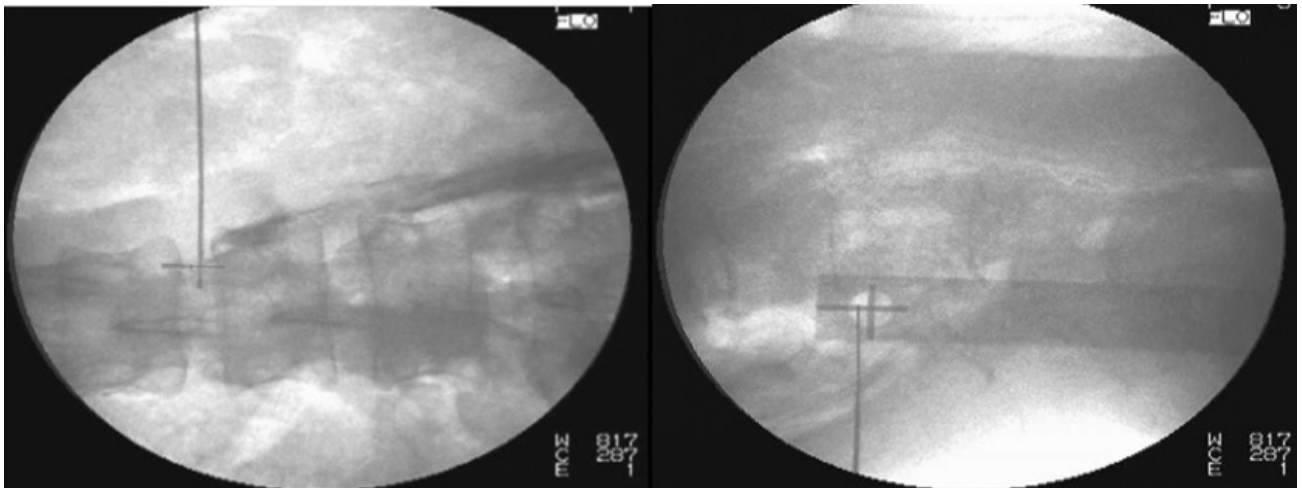


**Figure-8.** In each disc space, needle was directed through the Y' marker and inserted to the foramen. Needle was checked with fluoroscopy to be inside the Kambin Triangle. After obtaining desired angle to the skin entry, the needle and routing device was removed.

---

## DISCUSSION

Lumbar disc herniation is an important cause of back and leg pain. Although the number of patients increases with advanced age, epidemiological studies showed that incidence of intervertebral disc disease is increasing in younger ages. The percentage of people who have back pain at least once in their lives is 85%. Also, back pain is the second leading cause of referral to a doctor according to the statistics from North America and Western Europe <sup>(12)</sup>.

Patients who do not benefit adequately from conservative treatment methods constitute candidates for surgical treatment. Today, surgical interventions can be roughly divided into conventional discectomies and percutaneous methods. While microdiscectomy is the gold standard in conventional discectomies, percutaneous methods include chemonucleolysis, nucleoplasty, intradiscal electrothermal therapy, laser discectomy, and interlaminar or transforaminal endoscopic discectomy <sup>(11,14)</sup>. Neural tissue can be directly seen only in endoscopic discectomy within these percutaneous methods.

In the early 1980s, Kambin and Gellman developed a percutaneous arthroscopic approach. This method attracted attention and its use became widespread due to high patient comfort, less invasiveness, and similar success rate compared to microdiscectomy <sup>(5)</sup>. The procedure can be performed under general or local anesthesia. In addition, with the development of instrument and devices, such as high resolution, even three-dimensional imaging systems, automatic aspirators, special shaped high speed drills, radiofrequency bipolar cautery, the endoscopic approach became safer <sup>(8)</sup>.

There are some differences between microdiscectomy and endoscopic discectomy in terms of indications due to the characteristics of anatomical structures. If the sequestered disc's upper limit passes the lower border of the cranial pedicle, or the lower limit of sequestered part passes the middle of caudal pedicle, or most of the disc material is involved in the spinal canal, endoscopic transforaminal approach is not preferred. In addition, iliac wings disallow transforaminal approach due to closure of foramen in L5-S1, sometimes L4-L5 disc spaces. In far lateral disc herniation, FELD via TF approach gains an advantage over microdiscectomy in decompression of nerve root in extraforaminal region. However, microdiscectomy is gold standard when the disc is calcified or displaced into the spinal canal <sup>(9)</sup>. However, different surgeons have different techniques in line with their experience and use of high-tech devices. Nonetheless, the basis for the success of the operation is recognition of anatomical triangle in intervertebral foramen defined by Kambin. In recent years, the target of the percutaneous intervention

has shifted from middle of the disc space to the part of disc underneath the herniated part. This causes the skin entrance point to become more lateral, and it makes protection of anatomical structures more difficult and important. In this study, we aimed to develop and evaluate the effectiveness of a device that will provide access to these triangles without damaging surrounding tissues.

Until now, various methods have been described which are based on the help of imaging devices such as C-arm fluoroscopy, biplanar fluoroscopy, and CT, or totally free estimation to determine the entrance point, entrance angle, and target <sup>(7)</sup>.

Ahn et al. showed that more medial entrance point (6-9 cm lateral from midline) and steeper entrance angle (35-45°) are safer in transforaminal approach in upper levels compared to lower levels in lumbar disc herniations of 45 patients with the help of C-arm fluoroscopy <sup>(1)</sup>. Kim et al. used endoscopic transforaminal approach in 295 patients, entrance point (usually 10-14 cm lateral to midline) and angle were calculated with the help of preoperative abdominal CT. They were directed to medial pedicular line in AP view in disc herniation without ligamentous tear. They changed the entrance site more laterally in extruded/sequestered disc herniation. This series was compared by the authors with the patients who underwent microscopic discectomy by same authors. They found no significant difference between two groups in terms of success and complication rates <sup>(7)</sup>. Kafadar et al. used abdominal CT for preoperative evaluation in 42 patients who underwent endoscopic transforaminal approach. Entrance point (8-10 cm lateral to midline) and angle were calculated with the help of abdominal CT and checked with fluoroscopy during procedure. There were no neural, vascular or intraabdominal complications <sup>(4)</sup>.

Ruetten et al., who preferred accessing to spinal canal more tangentially, recommended performing abdominal and thoracic CT before surgery of upper lumbar disc spaces <sup>(9)</sup>. Peng et al. used an entrance point 12-14 cm lateral to midline, and targeted medial pedicular line in AP view, and posterior vertebral line in lateral view. Their complication rates were a bit higher than rates in previous studies (3.6% to 2.6%). On the other hand, an intramuscular psoas hematoma, which was large enough to cause hypovolemic shock in patient, was also reported recently in an endoscopic transforaminal L4-L5 discectomy performed under C-arm fluoroscopy <sup>(6)</sup>.

In our study, we performed abdominal CT before operation and used our special design routing device during operation. The most appropriate angle to midpedicular line for each disc space from skin entrance point (8-16 cm lateral to midline) without damaging retroperitoneal structures was calculated

with help of preoperative abdominal CTs. This calculation was performed in L1-L2, L2-L3, L3-L4, L4-L5 disc spaces. It was seen that in upper levels such as L1-2, L2-3, distance from midline was shorter and the foraminal entrance angle was increased compared to L3-L4, L4-L5 levels. We concluded that abdominal CT should be performed before operation for calculation of entrance angle to protect retroperitoneal structures especially in L1-L2, L2-L3, L3-L4 disc herniation. Anatomic variations (lumbarisation, sacralisation) which were not recognized in C-arm fluoroscopy and may cause misdiagnosis, were also detected in abdominal CTs of cadavers.

TF endoscopic discectomies were performed with routing device using calculated entrance points and angles. Although neural foramen was larger in upper lumbar levels, it was seen that the diameter of nerve root was smaller and the angle between root and dura was narrower. For this reason, we think that exiting root injury may occur during placement of working cannula, and traversing root injury may occur during removal of ligamentous complex in upper lumbar disc spaces.

Kambin triangle was reached successfully and safely with applying data obtained from CT ( $X', \alpha$ ) and C-arm fluoroscopy ( $X, Y, Y'$ ) to  $X, Y,$  and  $Y'$  markers of routing device's. There was  $Y'$  marker with protractor on routing device, and the metal rod on this  $Y'$  marker had an opening through which only the puncture needle could pass. This rod helped to reach the target. Also, the metal bar's back and forth movement and fixation to this mechanism contributed to operation of device. Entrance point and angle computed from CT were found to be compatible with the images obtained from fluoroscopy and endoscopy during operation.

Our specially designed routing device has achieved a definite success and safety during operation with the help of calculated entrance point and angle from abdominal CT images. For these reasons, we think our device will be very useful for clinical use.

## CONCLUSION

Conventional microsurgical methods and endoscopic interventions have now similar success rates. However, the advantage of reduction in tissue trauma provided by endoscopic methods cannot be denied. Our study with fresh cadavers has also shown that endoscopic transforaminal approach can be performed safely when appropriate anatomical signs are observed and especially when our CT-based routing device is used. However, it should be noted that open surgery is also an important part of spinal surgery and

surgeons must be fully qualified to cope successfully with the complications of endoscopic surgery, if necessary.

## REFERENCES

1. Ahn Y, Lee S-H, Lee JH, Kim JU, Liu WC. Transforaminal percutaneous endoscopic lumbar discectomy for upper lumbar disc herniation: clinical outcome, prognostic factors, and technical consideration. *Acta Neurochir (Wien)*. 2009;151(3):199-206.
2. Akçakaya MO, Yörükoğlu AG, Aydoseli A, et al. Serum creatine phosphokinase levels as an indicator of muscle injury following lumbar disc surgery: Comparison of fully endoscopic discectomy and microdiscectomy. *Clin Neurol Neurosurg*. 2016;145:74-78.
3. Fan G, Guan X, Sun Q, et al. Puncture Reduction in Percutaneous Transforaminal Endoscopic Discectomy with HE's Lumbar Location (HELLO) System: A Cadaver Study. *PLoS One*. 2015;10(12):e0144939.
4. Kafadar A, Kahraman S, Akbörü M. Percutaneous endoscopic transforaminal lumbar discectomy: a critical appraisal. *Minim Invasive Neurosurg MIN*. 2006;49(2):74-79.
5. Kambin P, Schaffer JL. Percutaneous lumbar discectomy. Review of 100 patients and current practice. *Clin Orthop*. 1989;(238):24-34.
6. Kim HS, Ju CI, Kim SW, Kim JG. Huge Psoas Muscle Hematoma due to Lumbar Segmental Vessel Injury Following Percutaneous Endoscopic Lumbar Discectomy. *J Korean Neurosurg Soc*. 2009;45(3):192-195.
7. Kim M-J, Lee S-H, Jung E-S, et al. Targeted percutaneous transforaminal endoscopic discectomy in 295 patients: comparison with results of microscopic discectomy. *Surg Neurol*. 2007;68(6):623-631.
8. Mathews HH. Transforaminal endoscopic microdiscectomy. *Neurosurg Clin N Am*. 1996;7(1):59-63.
9. Ruetten S, Komp M, Merk H, Godolias G. Full-endoscopic interlaminar and transforaminal lumbar discectomy versus conventional microsurgical technique: a prospective, randomized, controlled study. *Spine*. 2008;33(9):931-939. doi:10.1097/BRS.0b013e31816c8af7.
10. Sencer A, Yorukoglu AG, Akçakaya MO, et al. Fully endoscopic interlaminar and transforaminal lumbar discectomy: short-term clinical results of 163 surgically treated patients. *World Neurosurg*. 2014;82(5):884-890. doi:10.1016/j.wneu.2014.05.032.
11. Smith L. Chemonucleolysis. Personal history, trials, and tribulations. *Clin Orthop*. 1993;(287):117-124.
12. Tzaan W-C. Transforaminal percutaneous endoscopic lumbar discectomy. *Chang Gung Med J*. 2007;30(3):226-234.
13. Yörükoğlu AG, Göker B, Tahta A, et al. Fully endoscopic interlaminar and transforaminal lumbar discectomy: Analysis of 47 complications encountered in a series of 835 patients. *Neurocir Astur Spain*. May 2017. doi:10.1016/j.neucir.2017.03.003.

- 
14. Yörükođlu AG, Tahta A, Akçakaya MO, et al. Percutaneous Fully Endoscopic İnterlaminar Approach to the Filum Terminale: A Cadaveric Study. *World Neurosurg.* 2016;92:402-406. doi:10.1016/j.wneu.2016.05.055.